iScience, Volume *23*

Supplemental Information

ADAMTS18 Deficiency Leads to Pulmonary Hypoplasia and Bronchial Microfibril Accumulation

Tiantian Lu, Xiaotian Lin, Yi-Hsuan Pan, Ning Yang, Shuai Ye, Qi Zhang, Caiyun Wang, Rui Zhu, Tianhao Zhang, Thomas M. Wisniewski, Zhongwei Cao, Bi-Sen Ding, Suying Dang, and Wei Zhang

Supplemental Figures

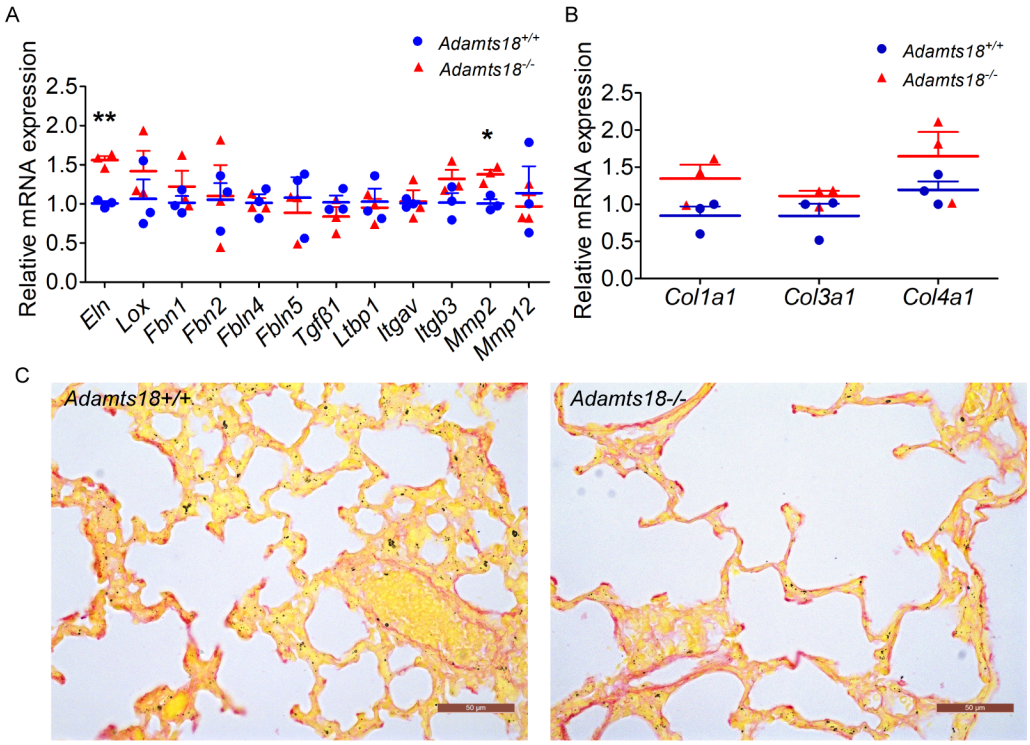

Figure S1. Effect of *Adamts*18 on elastin and collagen in the lungs of two-week-old mice, related to Figure 3 and Table S5. **A)** qRT-PCR results of key proteins involved in elastic fiber synthesis, assembly, and degradation, including *Tropoelastin (Eln)*, *Lox*, *Fibrillin 1 (Fbn1)*, *Fibrllin 2 (Fbn2)*, *Fibulin 4 (Fbln4)*, *Fibulin 5 (Fbln5)*, *Tgfβ1*, *Ltbp1*, *Integrin α5 (Itgα5)*, *Integrin β3 (Itgα3)*, *Mmp2*, and *Mmp12*. **B)** *q*RT-PCR results of *Col1a1*, *Col3a1,* and *Col4a1*. **C)** Lung collagen revealed by Sirius red staining. Scale bar, 50 µm. The relative quantity of target mRNA was normalized to that of the housekeeping gene *Gapdh* using the *ΔΔCt* method. Data are expressed as mean ± s.d. Statistical significance: **P* < 0.05; ***P* < 0.01

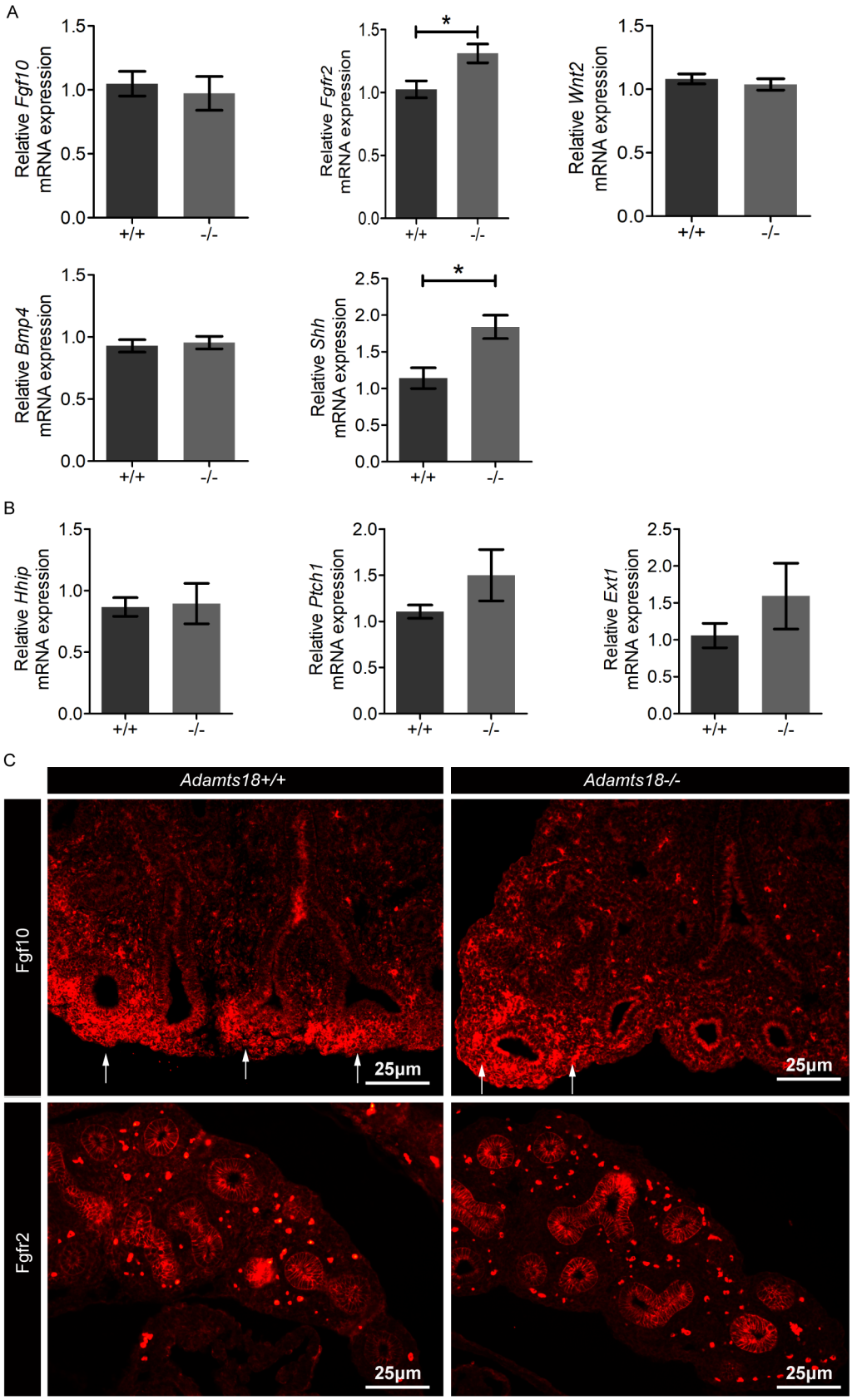

Figure S2. FGF10, Wnt2, Bmp4 and Shh signaling activity in the lungs of *Adamts18*$^{+/+}$ and *Adamts18*$^{-/-}$ mice, related to Figure 2, Table S4 and S5. A-B) Relative mRNA levels of *Fgf10*, *Fgfr2*, *Wnt2*, *Bmp4*, *Shh*, *Hhip*, *Ptch1*, and *Ext1*

determined by *q*RT-PCR. The relative quantity of target mRNA was normalized to that of the housekeeping gene *Gapdh* using the *ΔΔCt* method. Data are expressed as mean ± SEM. **C)** Representative immunostaining images of Fgf10 and Fgfr2 in E14.5 lungs from *Adamts18*$^{+/+}$ and *Adamts18*$^{-/-}$ mice. Scale bar, 25 µm.

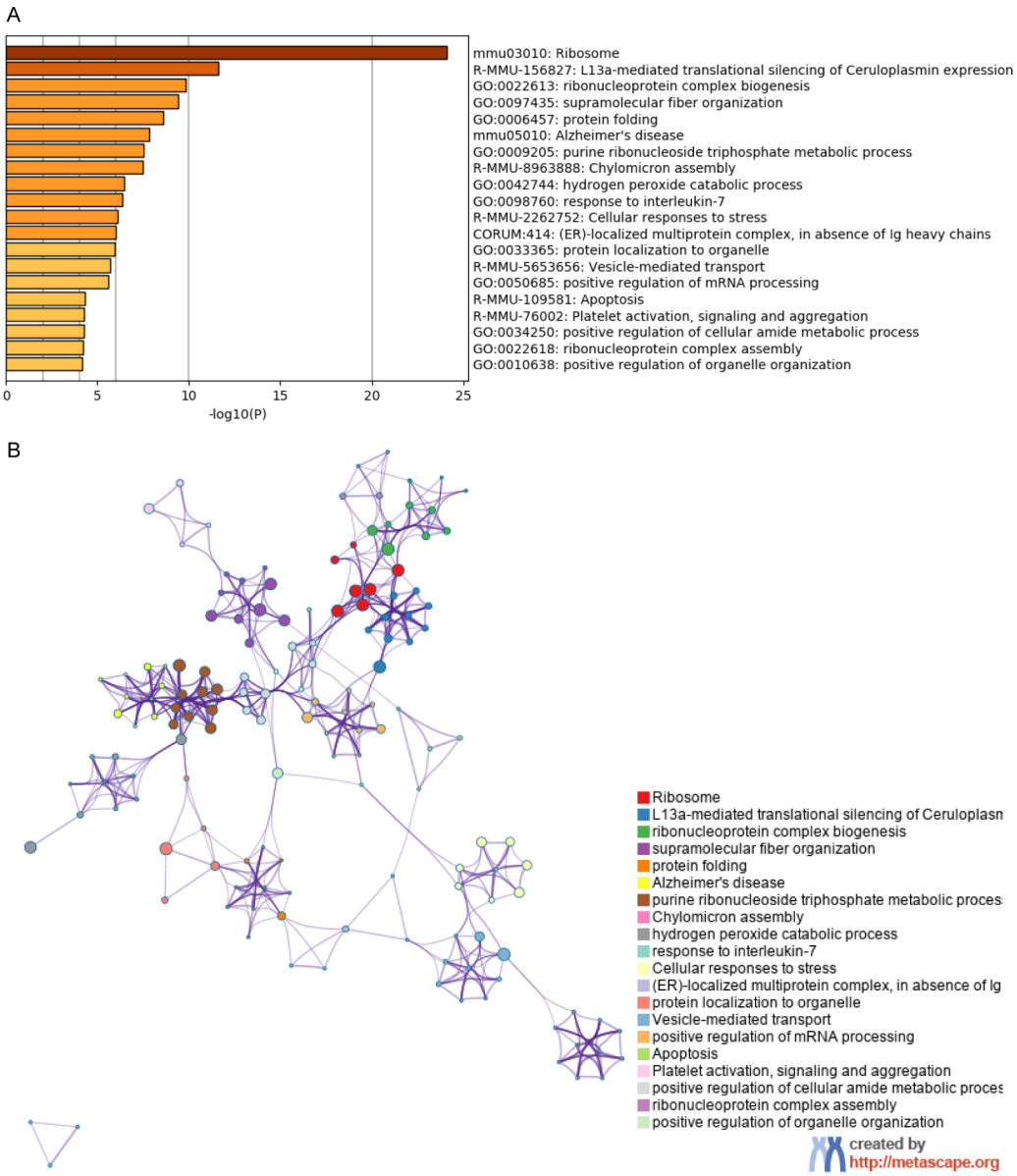

Figure S3. Related to Figure 6. A) Gene ontology (GO) term and pathway analysis. **B)** Protein-protein interactome network analysis of differentially expressed proteins by Metascape.

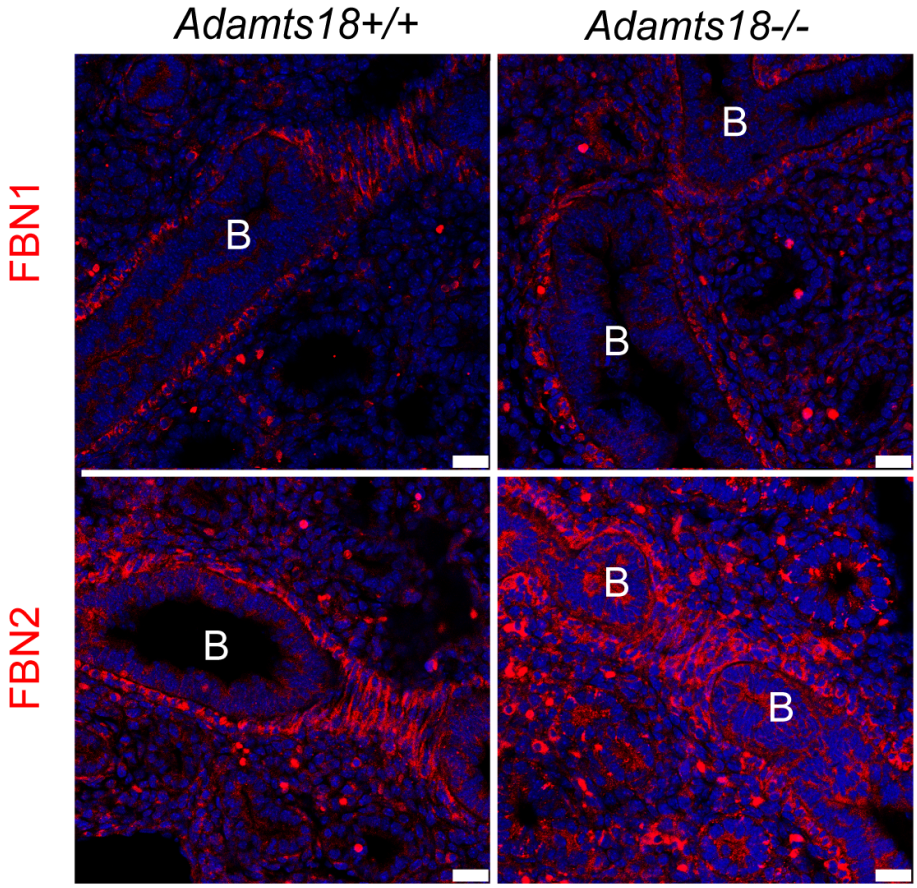

Figure S4. Immunohistochemical localization of fibrillin1 (FBN1) and FBN2 around E14.5 large airways, related to Figure 6 and Table S4. B: bronchi. Scale bar = 200 μm.

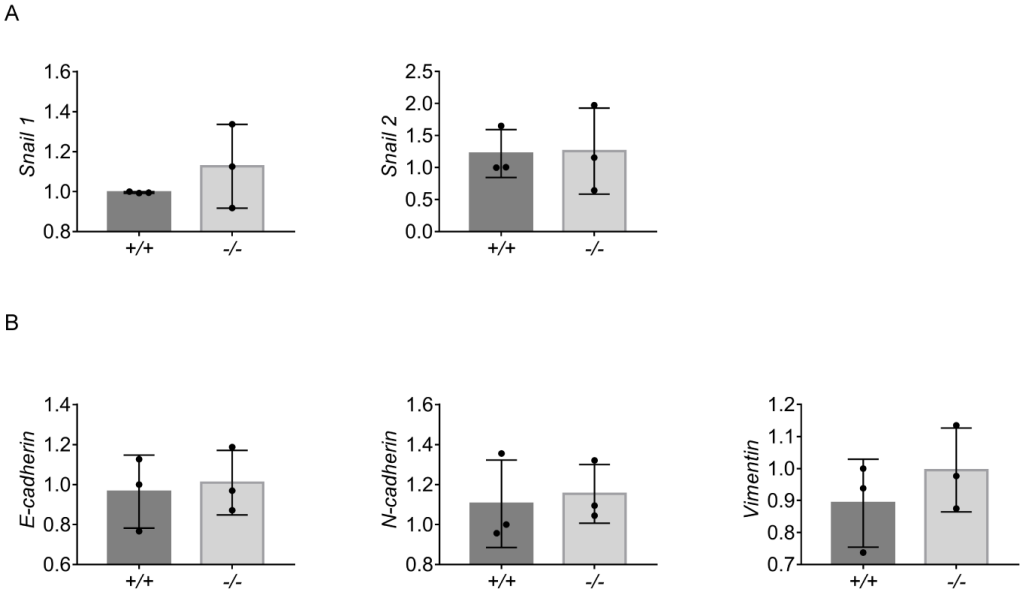

Figure S5. Epithelial–mesenchymal transition (EMT) signaling in the lungs of

***Adamts18*$^{+/+}$ and *Adamts18*$^{-/-}$ mice, related to Figure S3 and Table S5. A-B)**.
Relative mRNA levels of *Snail 1, Snail 2* **(A)**, *E-cadherin (Cdh1)*, *N-cadherin (Cdh2)*, and *Vimentin (Vim)* **(B)** Determination of mRNA levels by *q*RT-PCR. The relative quantity of target mRNA was normalized to that of the housekeeping gene *Gapdh* using the *ΔΔCt* method. Data are expressed as mean ± SEM.

Supplemental Tables

Table S1. Lung functions of 12-week-old mice, related to Figure 3.

	Male			Female		
	Adamts18$^{+/+}$ (n = 6)	*Adamts18*$^{-/-}$ (n = 6)	P value	*Adamts18*$^{+/+}$ (n = 6)	*Adamts18*$^{-/-}$ (n = 6)	P value
Ti (s)	0.23 ± 0.03	0.23 ± 0.08	0.95	0.33 ± 0.09	0.31 ± 0.11	0.94
Te (s)	0.12 ± 0.01	0.12 ± 0.02	0.73	0.12 ± 0.01	0.15 ± 0.04	0.59
f/min	172.16 ± 22.60	184.98 ± 57.09	0.62	136.67 ± 22.87	143.62 ± 53.72	0.78
Phigh (cmH_2O)	25.89 ± 0.34	25.81 ± 6.15	0.75	26.91 ± 0.63	27.26 ± 0.53	0.33
Pmean (cmH_2O)	6.20 ± 0.08	6.15±0.13	0.45	6.42 ± 0.15	6.50 ± 0.15	0.42
TVb (μL)	1.4 ± 0. 2	1.6 ± 0. 2	0.31	1.1 ± 0. 2	1.3 ± 0. 2	0.18
MVb (mL)	0.24 ± 0.05	0.30 ± 0.13	0.37	0.15 ± 0.04	0.19 ± 0.10	0.42
PIF/PEF (mL/s)	0.0111 ± 0.0021	0.0135 ± 0.0067	0.43	0.0078 ± 0.0012	0.0102 ± 0.0032	0.11

Ti: Time of inspiration; Te: time of expiration; f/min: frequency per minute; Phigh: airway pressure high; Pmean: airway pressure mean; TVb: tidal volume; MVb: minute volume; PIF/PEF: peak inspiratory/expiratory flow.

Table S2. 43 proteins involved in supramolecular fiber organization, related to Figure 8.

NO.	Genes	Protein Description	UniProtIds	Fold (5 *Adamts18*$^{-/-}$ /5 *Adamts18*$^{+/+}$)	P Value	AVG Ratio
1	Tmsb10	Thymosin beta-10	Q6ZWY8	0.303	0.029	1.723
2	Rpl13a	60S ribosomal protein L13a	P19253	0.691	<0.001	0.533
3	Fbn2	Fibrillin-2	Q61555	1.401	<0.001	0.486
4	Fbn1	Fibrillin-1	Q61554	1.295	0.001	0.373
5	Pfdn1	Prefoldin 1	Q9CQF7	0.779	0.046	0.360
6	Col1a2	Collagen alpha-2(I) chain	Q01149	1.283	0.037	0.360
7	Col3a1	Collagen alpha-1(III) chain	P08121	1.270	0.018	0.345
8	Tpm3	Tropomyosin alpha-3 chain	D3Z6I8;	0.824	<0.001	0.279
9	Apoe	Apolipoprotein E	P08226	0.825	0.021	0.278
10	Dpysl3	Dihydropyrimidinase-related protein 3	E9PWE8	1.195	0.049	0.257
11	Apoa1	Apolipoprotein A-I	Q00623	0.837	0.009	0.257
12	Arpc3	Actin-related protein 2/3 complex subunit 3	Q9JM76	0.863	0.013	0.213
13	Clu	Clusterin	Q06890	1.150	0.024	0.202
14	Rpl4	39S ribosomal protein L41, mitochondrial	Q9CQN7	1.128	<0.001	0.174
15	Lars	Leucine-tRNA ligase, cytoplasmic	Q8BMJ2	0.890	0.046	0.168
16	Arl2	ADP-ribosylation factor-like protein 2	Q9D0J4	0.891	0.027	0.167
17	Hist1h1b	Histone H1.5	P43276	0.894	0.001	0.162
18	Serpinf2	Alpha-2-antiplasmin	Q61247	0.909	0.034	0.138
19	Vim	Vimentin	P20152	0.916	0.017	0.127
20	Dync1h1	Cytoplasmic dynein 1 heavy chain 1	Q9JHU4	0.918	0.022	0.123
21	Apoa4	Apolipoprotein A-IV	P06728	0.924	0.029	0.114
22	Psmc4	26S proteasome regulatory subunit 6B	P54775	0.925	0.019	0.112
23	Hsp90ab1	Heat shock protein HSP 90-beta	P11499	0.932	0.024	0.102
24	Sptan1	Spectrin alpha chain, non-erythrocytic 1	P16546	0.933	0.002	0.100
25	Rdx	Radixin	P26043	0.934	0.012	0.099
26	Krt8	Keratin, type II	P11679	0.938	0.048	0.092

		cytoskeletal 8				
27	Hsp90b1	Endoplasmin	P08113	0.940	0.001	0.089
28	Add1	Alpha-adducin	Q9QYC0	1.057	0.014	0.080
29	Serpinh1	Serpin H1	P19324	0.952	0.001	0.071
30	Actn4	Alpha-actinin-4	P57780	0.953	0.014	0.069
31	Ran	GTP-binding nuclear protein Ran	P62827	0.959	0.020	0.060
32	Farp1	FERM, ARHGEF and pleckstrin domain-containing protein	F8VPU2	0.959	0.027	0.060
33	Myh10	Myosin-10	Q3UH59	0.964	0.017	0.053
34	Atp2a2	Sarcoplasmic/endoplasmic reticulum calcium ATPase 2	O55143	1.035	0.044	0.050
35	Rock2	Rho-associated protein kinase 2	A0A1Y7VMN0	1.034	0.040	0.048
36	Acta2	Actin, aortic smooth muscle	P62737	0.968	0.008	0.047
37	Mapk1	Mitogen-activated protein kinase 1	P63085	0.972	0.044	0.041
38	Hspa8	Heat shock cognate 71 kDa protein	P63017	0.981	0.016	0.028
39	Kif2c	Kinesin-like protein KIF2C	Q922S8	0.984	0.038	0.023
40	Hist1h1d	Histone H1.3	P43277	0.984	0.001	0.023
41	Map1b	Microtubule-associated protein 1B	P14873	1.016	0.013	0.023
42	Sec24b	Sec24-related gene family, member B (S. cerevisiae)	Q80ZX0	0.986	0.05	0.020
43	Arhgef2	Rho guanine nucleotide exchange factor 2	H3BJ40	0.99	0.044	0.014

AVG: Absolute value of Log2

Table S3. Quantification of important ECM proteins involved in branching morphogenesis in E14.5 lungs, related to Figure 6.

UniProtIds	Gene	Protein Description	mRNA		Protein	Subcellular Location
			H* (3 *Adamts18*$^{-/-}$ /2 *Adamts18*$^{+/+}$)	J* (3 *Adamts18*$^{-/-}$ /3 *Adamts18*$^{+/+}$)	MS (5 *Adamts18*$^{-/-}$ /5 *Adamts18*$^{+/+}$)	
P11087	Col1a1	Collagen alpha-1(I) chain	1.01	1.07	1.36	Extracellular matrix
Q01149	Col1a2	Collagen alpha-2(I) chain	0.96	1.14	1.28 (p = 0.037)	Extracellular matrix
P08121	Col3a1	Collagen alpha-1(III) chain	1.01	1.10	1.27 (p = 0.018)	Extracellular matrix
P11276	Fn1	Fibronectin	1.22	1.23	0.93	Extracellular matrix
P19137	Lama1	Laminin subunit alpha-1	1.25 (p = 0.022)	1.36	0.82	Basement membrane
Q61789	Lama3	Laminin subunit alpha-3	1.60 (p = 0.014)	1.64 (p = 0.016)	0.75	Basement membrane
Q61001	Lama5	Laminin subunit alpha-5	1.17	1.53	0.89	Basement membrane
P02469	Lamb1	Laminin subunit beta-1	1.29 (p = 0.008)	1.29 (p = 0.015)	0.97	Basement membrane
P02468	Lamc1	Laminin subunit gamma-1	1.32 (p = 0.042)	1.26	0.98	Basement membrane
Q3V3R4	Itga1	Integrin alpha-1	0.92	1.28	1.09	Membrane
Q62469	Itga2	Integrin alpha-2	1.15	1.19	1.06	Membrane

Q62470	Itga3	Integrin alpha-3	1.12	1.24	0.99	Membrane
P43406	Itgav	Integrin alpha-v	-	0.98	0.99	Membrane
Q61739	Itga6	Integrin alpha-6	0.95	1.37	1.11	Membrane
P09055	Itgb1	Integrin beta-1	-	0.94	0.99	Membrane
A2A863	Itgb4	Integrin beta-4	0.81	1.77	-	Membrane
P18828	Sdc1	Syndecan-1	1.21	-	-	Extracellular matrix
O35988	Sdc4	Syndecan-4	1.10	-	-	Extracellular matrix
Q62165	Dag1	Dystroglycan	1.10	1.28* (P = 0.050)	1.3	Basement membrane
P10493	Nid1	Nidogen-1	1.18	1.27 (P = 0.007)	0.99	Basement membrane
P33434	Mmp2	72 kDa type IV collagenase	0.78	-	0.97	Extracellular matrix
P29268	Ctgf	CCN family member 2	0.92	1.51 (P = 0.036)	-	Extracellular matrix
P04202	Tgfb1	Transforming growth factor beta-1 proprotein	0.84	1.02	-	Extracellular matrix

*H and J represent mice from two different littermates.

"-": mean data unavailable because of limited quantity of samples in real-time *q*PCR experiments or undetectable in MS analysis.

Table S4. Antibodies used in this study, related to Figure 4, 6, 8, S2, and S4.

Name	Catalog number	Company	Application (dilution)
Anti-MYC	TA150121	Origene	ICC (1:100)
Anti-Fibrillin1	Ab53076	Abcam	ICC (1:100)
Anti-DDK	TA150078	Origene	WB (1:5000)
Anti-FBN1-C ternimal	LS-C358981	LifeSpan Bioscience	WB (1:400)
Anti-FBN2	Sc-393968	Santa Cruze	WB (1:200)
Anti-FBN2	20252-1-AP	Proteintech	IHC (1:200)
Anti-FAK	AF6397	Affinity	IHC (1:100)
Anti-PFAK(Tyr397)	AF3398	Affinity	IHC (1:100)
Anti-TMSB10	TA351779	Origene	IHC (1:50)
Anti-Fgf10	GTX55619	Genetex	IHC (1:100)
Anti-Fgfr2	23328	CST	IHC (1:200)
Anti-CD11b	Ab133357	Abcam	IHC (1:2000)
Anti-MPO	AF3667	R&D system	IHC (1:40)
Anti-Histone H3	NB100-57135	Novus	IHC (1:200)
CY^{TM}3 Affinity Goat Anti-Rat IgG	112-165-003	Jackson Immuno Research	IHC/ICC (1:200)
CY^{TM}3 Affinity Goat Anti-Rabbit IgG	111-165-003	Jackson Immuno Research	IHC/ICC (1:200)
Alexa Fluor 488 Donkey Anti-Rabbit IgG	705-545-147	Jackson Immuno Research	IHC (1:200)
Alexa Fluor 647 Donkey Anti-Goat IgG	711-605-152	Jackson Immuno Research	IHC (1:200)

Table S5. Primers for quantitative real-time RT-PCR (*q*RT-PCR), related to Figure 1, 4, 5, 6, S1, S2, and S5.

Gene	Forward (5' to 3')	Reverse (5' to 3')
Gapdh	*GTGGAGTCATACTGGAACATGTAG*	*AATGGTGAAGGTCGGTGTG*
Adamts18	CCTCAAGTTGTCTGCTCCATCA	GCTGAAGAAATCCACGCAAGA
Fbn1	GCCAGAAAGGGTACATCGG	ACACACCTCCCTCCGTT
Fbn2	GTGAAACCACACAGAAATGTGAA	GAACAGTCGCCAGTCTCAC
Eln	CTGCTGCTAAGGCTGCTAAG	CCACCAACACCAGGAATGC
Lox	TCTTCTGCTGCGTGACAACC	GAGAAACCAGCTTGGAACCAG
Fbln4	CTCTGGGCGTTTCTGCTGTT	GCCATCTGTGCATTCCGTGT
Fbln5	GGGCTCATACTTCTGCTCG	GATGGTGAATGGCTGGTCT
Tgfb1	CTCCCGTGGCTTCTAGTGC	GCCTTAGTTTGGACAGGATCTG
Ltbp1	GGTTATTTGCCATCTTCCGTGTA	GAAATTTGGAGGGCACTGACA
Itgav	GGCACAAAGACCGTTGAGTA	ACCAGGACCACCGAGAAGTA
Itgb3	AGGGCAGTCCTCTATGTGGT	CTTGGCTCTGGCTCGTTCT
Mmp2	GACCATGCGGAAGCCAAGA	TGTGTAACCAATGATCCTGTATGTG
Mmp12	CACAGGAGGAACTATGAGTAGCA	AGGCAGACCAGGACACAGA
Col1a1	CGGTGCTACTGGAGTTCAAGGT	CAGGGAAACCACGGCTACCA
Col3a1	CCACAAGGATTACAAGGCATACC	TCCAGGAGCACCGACTTCA
Col4a1	AATGGCATTGTGGAGTGTCAAC	TTCTGTCCAACTTCACCTGTCAA
Fgf10	TCCGTACAGTGTCCTGGAGATA	CCCTTCTTGTTCATGGCTAAGTAAT
Fgfr2	CGCTTCATCTGCCTGGTCTTG	ACGGTGCTCCTTCTGGTTCTAA
Wnt2	CCTGATGAACCTTCACAACAACA	GCCACTCACACCATGACACT
Bmp4	AGCCCGCTTCTGCAGGA	AAAGGCTCAGAGAAGCTGCG
Shh	CTCCGAACGATTTAAGGAACTCAC	GCCACTGGTTCATCACAGAGAT
Hhip	GGAGCCTTACTTGGACATTCAC	CCGTTCCTGGTTGGTGGTAT
Ptch1	CTCAGGCAATACGAAGCACAG	GGAGGCTGATGTCTGGAGTC
Ext1	GTTGCCATTCTCCGAAGTGATT	TGTGTCTGCTGTCTAAGTGCTA
Col1a2	CGATGTTGAACTTGTTGCTGAG	GGCAGGCGAGATGGCTTAT
Fn1	AAGAGAAGACAGGACCAATGAA	TTGAGAGCATAGACACTGACTT
Lama1	GCTATCCTGCCCACATCAAAC	CAAGGACTGCACTTGTGAGC
Lama3	CTCCAATGACCTCAGTCCAGAA	TCTCAGAACGATGCGGAACA
Lama5	TTGGAGAATGGCGAGATTGTG	CGAAGTAACGGTGAGTAGGAGA
Lamb1	TCTGTGAACCATGTACCTGTGA	GACACTGACCAGCAATGAGAC
Lamc1	TGCCGCCAATGTGTCAATC	TGCCACTCGTACAATGTCATC
Sdc1	CTGGAGAACAAGACTTCACCTT	AGCACTTCCTTCCTGTCCAA
Sdc4	ACCTCCTGGAAGGCAGATACT	GGCACCAAGGGCTCAATCA
Dag1	GAGTGAGCATTCCAACGGATT	CAGTGTAGCCAAGACGGTAAG
Ctgf	AAGGACCGCACAGCAGTT	AGTTGGCTCGCATCATAGTTG
Nid1	AGAGCAACGGAGCCTATAACAT	CGGTAGCAGGACTTCCAATCT
Itga1	CGGCTTCAGTGCTCATTATTCA	ATGACCACAGTTCCGTTCCA
Itga2	CGCAAGAGACTACGCTTATTCA	CTCGCCATCGGTCACAACT
Itga3	AGAGACACATTGCCAGACACT	CGCAGAGGTAAGGAGTAGTTCA

Itga6	TCTCGTTCTTCGTTCCAGGTT	GCAGCAGCGGTGACATCTA
Itgb1	TGGTCAGCAACGCATATCTG	GTTACATTCCTCCAGCCAATCA
Itgb4	GACCAATGGCGAGATCACAG	TCCACGAGCACCTTCTTCATA
Snail1	GTCTGCACGACCTGTGGAAA	GGTCAGCAAAAGCACGGTTG
Snail2	TCATCCTTGGGGCGTGTAAG	GATGGCATGGGGGTCTGAAA
Cdh1	CAGCCGGTCTTTGAGGGATT	TGACGATGGTGTAGGCGATG
Cdh2	ACAGCGCAGTCTTACCGAAG	CTTGAAATCTGCTGGCTCGC
Vim	TTCTCTGGCACGTCTTGACC	GCTTGGAAACGTCCACATCG

Transparent Methods

Reagents

All reagents were purchased from Sigma–Aldrich (St. Louis, MO, USA) unless otherwise indicated. Primary antibodies used in this study are listed in Table S4.

Animals

Adamts18 knockout (*Adamts18*$^{-/-}$) and wildtype (*Adamts18*$^{+/+}$) mice with the C57BL/6/129Sv background were generated and genotyped as previously described (Lu et al., 2017). Animals were maintained on a 12-h light/dark schedule (lights on at 06:00) in a specific pathogen-free facility. All procedures for animal experiments were approved by the Institutional Animal Care and Use Committee of East China Normal University (ECNU).

RNA in situ hybridization

RNA in situ hybridization (ISH) was performed as described previously (Zhu et al., 2019). Briefly, mouse lungs were fixed in 10% neutral buffered formalin for 24 h at room temperature (RT) and paraffin-embedded following standard methods. ISH was performed on 5-μm-thick sections using the RNAscope 2.5 HD Reagent Kit-RED (Advanced Cell Diagnostics, Hayward, CA). Specific probes were used to detect target mRNAs as described (Zhu et al., 2019).

Quantitative Real-Time RT-PCR Analysis

Quantitative real-time RT-PCR (*q*RT-PCR) was performed using the Step One Plus real-time PCR system (ThermoFisher, Carlsbad, CA) with SuperReal PreMix Plus (SYBR Green; TIANGEN). Primers used are listed in Table S5. The relative quantity of target mRNA was determined using the *ΔΔCt* method, with *Gapdh* as the reference gene. All reactions were performed in triplicates.

Explant cultures

Lung explant cultures were performed as previously described (Moral and Warburton, 2009). Briefly, E11.5 lungs were cultured on Nucleopore polycarbonate track-etch membranes (WHA-110414, Whatman) at 37°C in a 5% CO_2 incubator for 72 h. For the rescue experiments, sense and antisense-phosphorothioated oligodeoxynucleotides (SODN and ASODN) were synthesized and added to the culture medium at the concentration of 0.5 μM for *Fbn1* or 1 μM for *Fbn2 (Kanwar et al., 1998; Yang et al., 1999)*. Sequences of the oligonucleotides are as follows: *Fbn1* sense ODN: 5'-GCCAGCGCGACCTCCAGCAGCCCTCCTCGCCGCAT-3', *Fbn1* aitisense ODN: 5'-ATGCGGCGAGGAGGGCTGCTGGAGGTCGCGCTGGC-3', *Fbn2* sense ODN: 5'-CTCGGAGTATTTCCTGCTGTCCTCGCCTGCGGAC-3', *Fbn2* antisense ODN: 5'-GTCCGCAGGCGAGGACAGCAGGAAATACTCCGAG-3'. The culture medium was refreshed every 24 h. Images of explants were taken using an Mshot microscope with MS60 camera (Guangzhou, China). The number of branches was counted manually, and the length of each airway was calculated by the software Image Pro

Plus 6.0 (IPP, Media Cybernetics, Inc., Silver Spring, MD, USA).

Lung cast

Mice were euthanized by CO_2 asphyxiation. The trachea was exposed just below the larynx, and a catheter was inserted and securely tied with braided silk surgical suture. The lungs were inflated with casting agent (90 ml ethyl acetate, 10 g polyvinyl chloride, 2.7 ml dibutyl phthalate, and appropriate amount of oil paints), separated from trachea, and transferred to a 60°C oven. After the casting agent was solidified, the lungs were immersed in 50% HCl to remove tissues (only airways left). Airways were imaged using an Mshot microscope.

Histology, immunohistochemistry, and immunofluorescence

Lung tissues were fixed in 10% neutral buffered formalin and embedded in paraffin. After dewaxing and rehydration, hematoxylin and eosin (HE) staining or Hart's staining was performed on 5-μm sections to determine radial alveolar counts (RAC) and elastin distribution. Immunohistochemical staining of sections was performed using anti-CD11b, anti-histone H3, anti-MPO, anti-FBN1, anti-FBN2, anti-PFAK (Tyr397), anti-FAK, anti-TMSB10, anti-FGF10, and anti-FGFR2 antibodies. For immunofluorescence examination, 48 h after transfection, the cells were fixed with pre-cooled ethanol for 20 min. The samples were incubated with anti-ddk (or anti-myc), anti-fibrillin1, and anti-fibrillin2 antibodies overnight at 4°C, followed by incubation with the secondary antibody. Samples were counterstained with DAPI (MP, Carlsbad, CA) and imaged with a Leica SP8 confocol microscope (Leica Microsystems, Wetzlar, Germany).

FITC-phalliodin staining

E14.5 lung tissues were obtained, embedded in optimal cutting temperature (OCT) compound, and cut into 10-μm thick sections with a Leica CM3050 S cryostat microtome (Leica Biosystem, Wetzlar, Germany). The sections were fixed for 15 min with 4% formaldehyde in PBS and permeabilized with 0.5% triton X-100 in PBS for 20 min, followed by incubation with 0.1 mg/ml FITC-phalloidin diluted in PBS containing 1% BSA at 37°C for 2 h and counterstaining with DAPI. After mounting on slides, the sections were examined with a Leica SP8 confocal microscope.

Lung function examination

Mice were anesthetized with a mixture of urethane (14% m/v), alpha-chloralose (0.7% m/v), and sodium tetraborate decahydrate (0.7% m/v) in saline and connected to a computer-controlled ventilator via the tracheal cannula. After normal respiratory movements were recorded, mice were mechanically ventilated with room air at 110 breaths per min with the expiration/inspiration ratio of 20:10. Pulmonary function tests were performed using the AniRes2005 Lung Function System (Bestlab Technology Co., Ltd).

LPS-induced acute lung injury

Lipopolysaccharide (LPS) was diluted to a final concentration of 1 mg/ml in normal saline. Anesthetized mice were injected intraperitoneally (I.P.) with LPS at 10 mg/kg. Lung tissues were collected at different time points (0 h, 3 h, 6 h, 12 h, and 24 h) after LPS injection. Pathological grade of lung injury was defined as follows: Grade 0, normal alveoli, alveolar septum, and bronchi; Grade 1, partial alveolar septal congestion; Grade 2, moderate alveolar septal congestion and intra-alveolar hemorrhage; Grade 3, severe congestion and bleeding in alveolar septum and alveoli. Frozen lung tissues (around 30 mg) were homogenized to measure IL-6 using a commercially available ELISA kits (LYBD Bio-Technique Co, Ltd, Beijing, China), and data were normalized to protein concentration measured by the bicinchoninic acid (BCA) method.

Bronchoalveolar lavage

Mice were sacrificed by CO_2 asphyxiation and bronchoalveolar lavaged 3 times, each with 0.8 ml of PBS via a 22G catheter. The bronchoalveolar lavage fluid (BALF) was centrifuged at 400 xg for 7 min at 4°C, and the pellet was resuspended in 20 µl PBS containing 1% BSA. The resuspended cells were placed on a slide, dried, stained with Diff-Quick (Solarbio Life Science, Beijing, China), and counted under a microscope at 100x magnification.

Bleomycin-induced lung fibrosis

Mice were anesthetized and intratracheally instilled with 100 µl of saline or bleomycin sulfate dissolved in saline (1 mg/kg body weight), followed with 300 µl of air to ensure delivery to the distal airways. Mouse mortality was monitored for 25 days after bleomycin injection. To assess lung fibrosis, mice were sacrificed, and lung tissues were examined microscopically at 100 x magnification. The severity of fibrosis was determined according to the method of Ashcroft et al (Ashcroft et al., 1988) and scored as follows: grade 0, normal lung; grade 1, minimal fibrous thickening of alveolar or bronchiolar walls; grade 3, moderate thickening of walls without obvious damage to lung architecture; grade 5, increased fibrosis with definite damage to lung structure and formation of fibrous bands or small fibrous masses; grade 7, severe distortion of structure and large fibrous areas; grade 8, total fibrous obliteration.

Proteomic analysis of embryonic lungs

Whole lung tissues from E14.5 embryos were digested with sequencing grade trypsin (Promega) and fractionated with high PH reversed phase chromatography. The data-independent acquisition (DIA) analysis was performed on an Orbitrap Fusion LUMOS mass spectrometer (Thermo Fisher Scientific) connected to an Easy-nLC 1200 via an Easy Spray (Thermo Fisher Scientific). The DIA raw files were analyzed in Spectronaut X (Biognosys, Schlieren, Switzerland). Pathway enrichment analysis was performed with MetaScape (http:// metascape.org/).

Transmission electron microscopy (TEM)
Distal parts of E14.5 lungs were fixed with 2.5% glutaraldehyde at 4°C, followed by fixation with osmium tetroxide, dehydration in alcohol, embedding in plastic, ultra-thin sectioning, flotation of the sections on aqueous medium, and staining with uranyl acetate and lead acetate. Images were taken with a Tecnai G2 Spirit BioTWIN transmission electron microscope (FEI, Hillsboro, Oregon).

ADAMTS18 and fibrillin1 (FBN1) expression
The plasmid for expression of Myc-DDK tagged mouse full-length *Adamts18* (pCMV6-*Adamts18*, the ORF clone with sequence NM_172466 in pCMV6-Entry) was purchased from Origene (Rockville, MD). Plasmid DNA was introduced into HEK293T cells by transfection using Lipofectamine 2000 (Invitrogen/Life technologies, Carlsbad, CA).

Co-Immunoprecipitation (IP)
Mouse dermal fibroblast cells (DFCs) and HEK293T cells were co-cultured and transiently transfected with pCMV6-*Adamts18* or empty vector. At 48 h, the cells were washed once with PBS and lysed in NP-40 buffer (50 mM Tris-base pH 7.5, 150 mM NaCl, 1% NP-400, and protease inhibitors). Cell lysates were incubated with anti-DDK agarose (TA150037, Origene, Rockville, MD) at 4°C overnight and washed with 1% NP40 washing buffer. The proteins eluted from the agarose beads were resolved by SDS-PAGE and analyzed by Western blotting with anti-fibrillin 1 C-terminal, anti-fibrillin 2, and anti-DDK (DYKDDDDK) primary antibodies and horseradish peroxidase (HRP)-conjugated secondary antibody. The immunoreactive bands were visualized with enhanced chemiluminescence (ECL) Western blot kit (Millipore, Boston, MA).

RhoA Activity
RhoA activity was detected using the Rho Activation Assay Biochem Kit (Cytoskeleton, Inc, Dencer, CO). Briefly, E15.5 lung tissues were isolated and homogenized in the lysis buffer. The cell lysate thus obtained was adjusted to 1 mg/ml of protein and then incubated with rhotekin-RBD beads at 4°C for 1 h. RhoA was then eluted from the rhotekin-RBD beads and analyzed by Western blotting with anti-RhoA antibody included in the kit.

Statistics
Data were analyzed by Student's *t* test or Log-rank (Mantel-Cox) test using the software package Prism version 7 (GraphPad, La Jolla, CA, USA). Data are shown as mean ± SEM or mean ± SD. A p value < 0.05 was considered statistically significant.

Supplemental Reference
Ashcroft, T., Simpson, J.M., and Timbrell, V. (1988). Simple method of estimating severity of pulmonary fibrosis on a numerical scale. Journal of clinical pathology *41*, 467-470.

Kanwar, Y.S., Ota, K., Yang, Q., Kumar, A., Wada, J., Kashihara, N., and Peterson, D.R. (1998). Isolation of rat fibrillin-1 cDNA and its relevance in metanephric development. The American journal of physiology *275*, F710-723.
Lu, T., Dang, S., Zhu, R., Wang, Y., Nie, Z., Hong, T., and Zhang, W. (2017). Adamts18 deficiency promotes colon carcinogenesis by enhancing beta-catenin and p38MAPK/ERK1/2 signaling in the mouse model of AOM/DSS-induced colitis-associated colorectal cancer. Oncotarget *8*, 18979-18990.
Mei, S.H., McCarter, S.D., Deng, Y., Parker, C.H., Liles, W.C., and Stewart, D.J. (2007). Prevention of LPS-induced acute lung injury in mice by mesenchymal stem cells overexpressing angiopoietin 1. PLoS medicine *4*, e269.
Moral, P.M.D., and Warburton, D. (2009). Explant culture of mouse embryonic whole lung, isolated epithelium, or mesenchyme under chemically defined conditions as a system to evaluate the molecular mechanism of branching morphogenesis and cellular differentiation. Methods Mol Biol *633*, 71-79.
Yang, Q., Ota, K., Tian, Y., Kumar, A., Wada, J., Kashihara, N., Wallner, E., and Kanwar, Y.S. (1999). Cloning of rat fibrillin-2 cDNA and its role in branching morphogenesis of embryonic lung. Dev Biol *212*, 229-242.
Zhu, R., Pan, Y.H., Sun, L., Zhang, T., Wang, C., Ye, S., Yang, N., Lu, T., Wisniewski, T., Dang, S.*, et al.* (2019). ADAMTS18 Deficiency Affects Neuronal Morphogenesis and Reduces the Levels of Depression-like Behaviors in Mice. Neuroscience *399*, 53-64.